**Effective Gating in Single-Molecule Junctions through Fano Resonances** 

Claudia R. Prindle<sup>1†</sup>, Wanzhuo Shi<sup>1†</sup>, Liang Li<sup>1</sup>, Jesper Dahl Jensen<sup>2</sup>, Bo W. Laursen<sup>2</sup>, Michael

L. Steigerwald<sup>1</sup>, Colin Nuckolls<sup>1\*</sup>, and Latha Venkataraman<sup>1,3\*</sup>

<sup>1</sup>Department of Chemistry, Columbia University, New York, New York 10027, United States

<sup>2</sup>Nano-Science Center and Department of Chemistry, University of Copenhagen,

Universitetsparken 5, 2100 Copenhagen, Denmark

<sup>3</sup>Department of Applied Physics and Applied Mathematics, Columbia University, New York,

New York 10027, United States

†equal contribution

Email: lv2117@columbia.edu, cn37@columbia.edu

**ABSTRACT:** 

The successful incorporation of molecules as active circuit elements relies on the ability to tune

their electronic properties through chemical design. A synthetic strategy that has been used to manipulate

and gate circuit conductance is attaching a pendant substituent along the molecular conduction pathway.

However, such a chemical gate has not yet been shown to significantly modify conductance. Here, we report

a novel series of triarylmethylium and triangulenium carbocations gated by different substituents coupled

to the delocalized conducting orbitals on the molecular backbone through a Fano resonance. By changing

the pendant substituents to modulate the position of the Fano resonance and its coupling to the conducting

orbitals, we are able to regulate the junction conductance by a remarkable factor of 450. This work thus

provides a new design principle to enable effective chemical gating of single-molecule devices towards

effective molecular transistors.

1

The conductance of single metal-molecule-metal devices originates from ballistic quantum tunneling, which is dictated by an energy dependent transmission probability around the Fermi energy  $(E_F)$  of the metal electrodes.<sup>1-4</sup> This transmission function comprises Lorentzian resonances derived from the frontier molecular orbitals (MOs) and energetically broadened by their coupling to the metal electrodes.<sup>5, 6</sup> When transmission is dominated by a single MO level – either the lowest unoccupied molecular orbital (LUMO) or the highest occupied molecular orbital (HOMO) – its energy dependence is given by the Breit-Wigner Lorentzian formula<sup>7, 8</sup>

$$T(E) = \frac{\Gamma^2}{(E - \varepsilon)^2 + \Gamma^2} \tag{1}$$

where E is the energy of the incident electron,  $\varepsilon$  is the energy of the MO and  $\Gamma$  is its broadening. Note that E and  $\varepsilon$  are relative to  $E_F$  which is set to zero. Chemical substituents on the molecular backbone can be used to alter  $\varepsilon$  to tune transmission and thus single-molecule junction conductance. However, this type of tunability is generally minimal in part because  $\varepsilon$  is often large 11-14 and gating does not change  $\Gamma$  significantly.

Charged species, such as cations (or anions) that have a low-lying LUMO (or HOMO) owing to their inherent tendency to attract electrons (or holes),  $^{15, 16}$  have the potential to be effectively gated by chemical substituents as they have a small  $\varepsilon$ . Chemical gating is even more effective when the substituent is not coupled to the metal leads, as illustrated in Figure 1a. In this case, the substituent alters the effective alignment and coupling of the conducting MO channel, thereby enabling a substantial tuning of conductance. The transmission function for such a system follows a modified Breit-Wigner formula  $^{17}$ 

$$T(E) = \frac{\Gamma^2}{\left(E - \varepsilon - \frac{t^2}{E - \varepsilon_p}\right)^2 + \Gamma^2}$$
 (2)

where the two additional parameters are  $\varepsilon_p$ , the energy level of the localized orbital on the substituent and t, its coupling to the molecular backbone. The substituent alters the transmission through a quantum

interference effect, which manifests as an asymmetric feature with a resonance (peak) and anti-resonance (dip) in the transmission function, otherwise known as a Fano resonance (Figure 1b). The Fano resonance alters the position of the conducting LUMO away from  $E_F$  (increasing  $\varepsilon$ ) while also weakening its coupling to the leads (decreasing  $\Gamma$ ) resulting in a lower junction conductance (Supporting Information Section 1). A molecular system comprised of such pendant substituents can thus alter the molecular junction conductance based on how strongly the pendant orbital is coupled to the conducting orbital, i.e., based on the magnitude of t (eq 2).

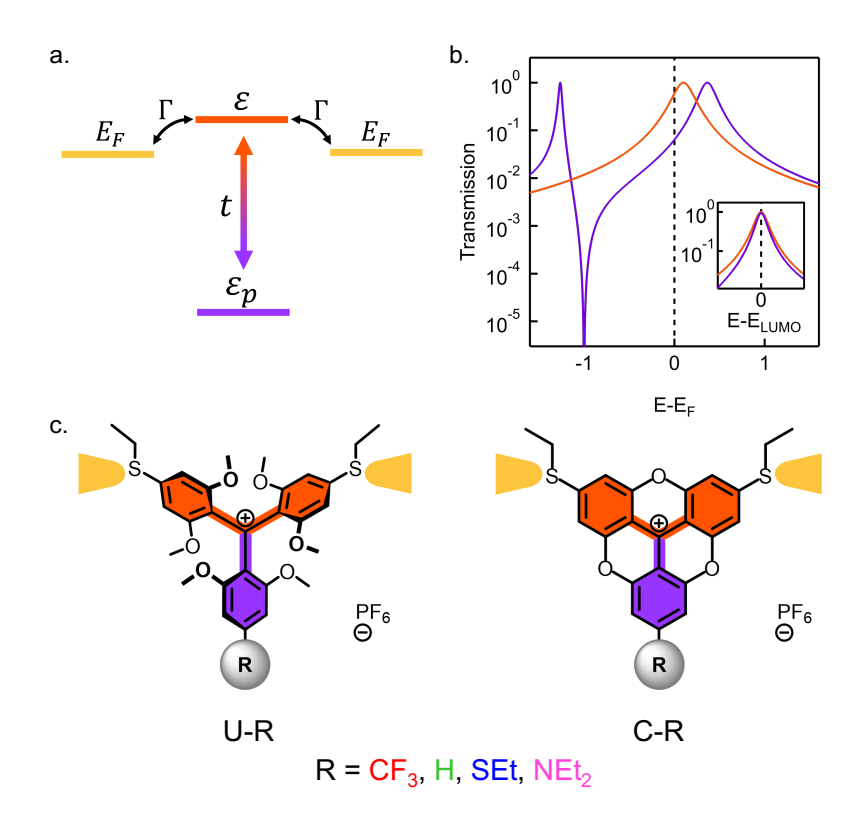


Figure 1. (a)  $\varepsilon$  (orange) and  $\varepsilon_p$  (purple) are the energy levels of the delocalized orbital (along a molecular conduction pathway) and the localized orbital (on a pendant substituent). (b) Model transmission function of the junction shown in (a) demonstrating quantum-interference effect that leads to a Fano resonance (purple, t=0.6,  $\varepsilon_p=-1$ ,  $\varepsilon=0.1$ ,  $\Gamma=0.06$ ). A single-level model (orange,  $\varepsilon=0.1$ ,  $\Gamma=0.06$ ) is also shown. Inset: LUMO resonances showing the narrowing of the Lorentzian peak due to the Fano resonance. c) Structures of the triarylmethylium (U-R) and triangulenium (C-R) series, where R represents a

substituent on the pendant phenyl ring ( $R = CF_3$ , H, SEt,  $NEt_2$ ). Ethanethiol linkers are installed at the ends of the main conduction pathway to allow Au-molecule-Au junction formation.

To test these ideas, we synthesized a series of uncyclized triarylmethylium (U-R) and cyclized triangulenium (C-R) analogs (Figure 1c) with different pendant electron withdrawing or donating substituents and showed that they impact single-molecule conductance significantly. <sup>18-20</sup> The syntheses are detailed in the Supporting Information Section 2. The U-R molecular series has propeller-like structures, whereas the C-R series has locked rigid planar structures. Both the U-R and C-R molecular series are terminated with two aurophilic thioethyl (SEt) substituents that serve as chemical anchor groups, as well as a third substituent of varying electron withdrawing or donating ability (R = CF<sub>3</sub>, H, SEt, NEt<sub>2</sub>) in order to assess the electronic effect of a pendant substituent on molecular conductance.

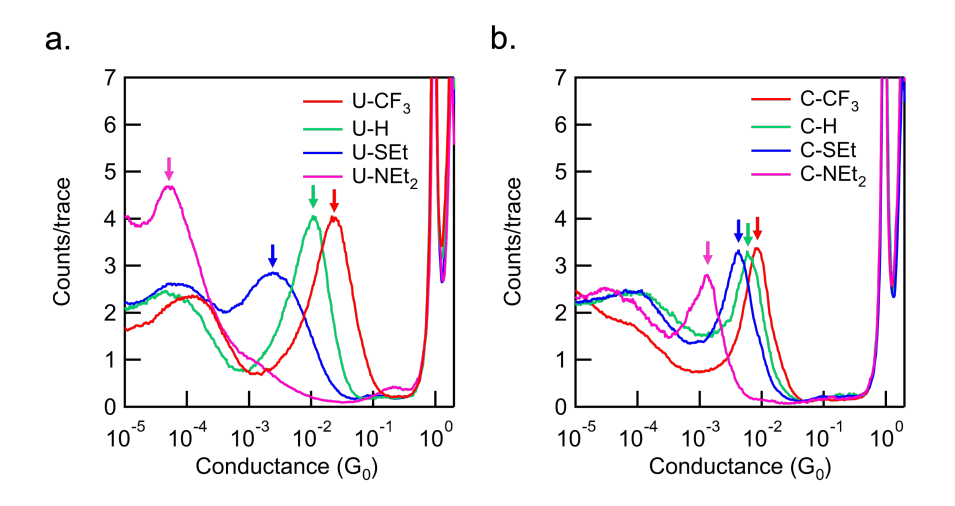


Figure 2. Logarithmically binned 1D conductance histograms for the (a) U-R and (b) C-R series. Each histogram is generated from over 5000 individual traces without any data selection. All measurements are made at a bias voltage of 100 mV.

We measure the molecular junction conductance of the U-R and C-R analogs with the scanning tunneling microscope-based break-junction (STM-BJ) technique.<sup>21, 22</sup> We use 100 µM solutions prepared in propylene carbonate (PC) or tetraethylene glycol dimethyl ether (TEGDME) and perform measurements at a bias voltage of 100 mV. The Au tips are coated with wax to suppress the capacitive and Faradaic

background current induced by the ionic solution.<sup>23</sup> We record over 5000 traces for each molecule, and compile these into one-dimensional (1D) conductance histograms without data selection. Sharp peaks at  $G_0$  indicate the formation of Au point contacts during the measurement, while the peaks below  $G_0$  are due to the formation of molecular junctions. By fitting the molecular peaks with a Gaussian function, we ascertained the most probable conductance values for the molecules being measured.

Figures 2a and 2b show the 1D conductance histograms collected for the U-R and C-R series, respectively. The corresponding two-dimensional conductance-displacement histograms are shown in Figure S4. In the U-R series, a continuous decrease in molecular conductance is observed as the pendant R group is changed from electron withdrawing (CF<sub>3</sub>) to electron donating (NEt<sub>2</sub>). The molecular conductance of U-CF<sub>3</sub> is a remarkable 450 times higher than that of U-NEt<sub>2</sub>. However, while the trend of decreasing molecular conductance is the same for the C-R series, the impact is much less. We see a factor of 6 decrease in the conductance of the C-R analogs going from the CF<sub>3</sub> substituent to the NEt<sub>2</sub> substituent. The exceptional conductance shift in the U-R series due to chemical gating shows clearly the impact of a pendant substituent on conductance. By contrast, chemical gating  $^{11-14}$  that simply shift the conducting orbital yields much smaller changes (<15) in conductance similar to what is observed in the C-R series. There is a second peak aroung  $10^{-4}G_0$  which is not as sharp and high-conducting as that of the junctions formed by single cation. We hypothesis that this lower-conducting peak represents a junction attached with a solvent dipole/counterion.

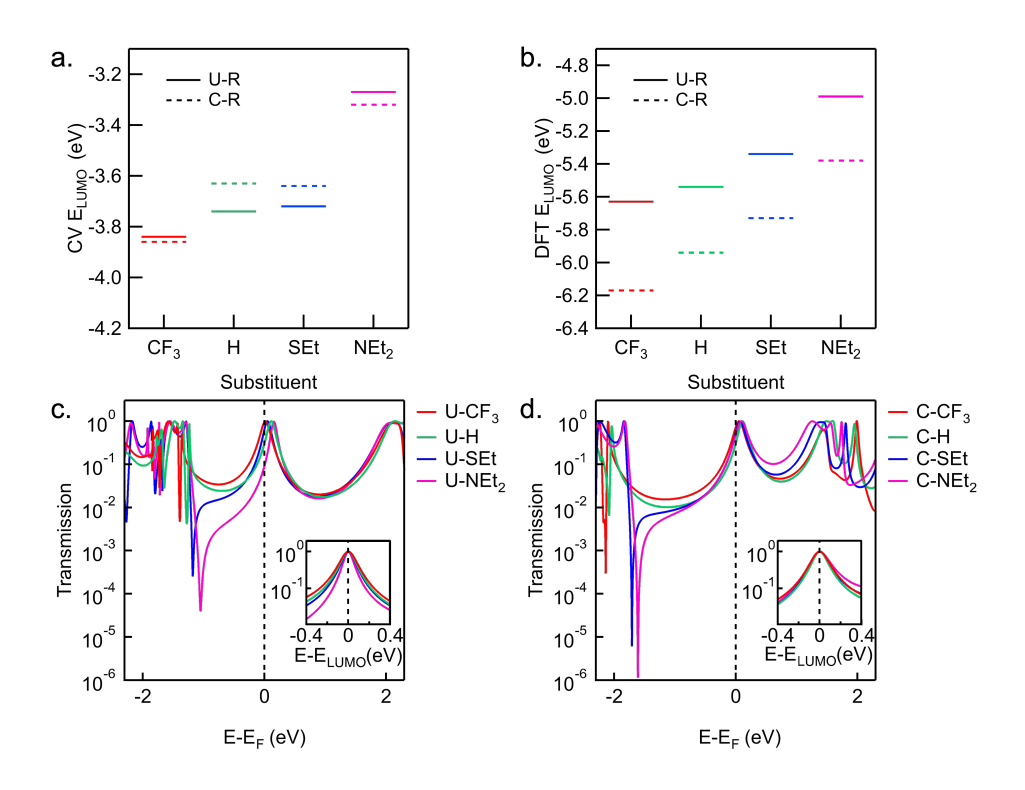


Figure 3. (a) LUMO energies of the U-R and C-R series derived by CV. (b) LUMO energies of the (c) U-R and (d) C-R series DFT calculation. Transmission functions of the U-R and C-R series.  $E_F$  is marked with a dashed line. Inset: LUMO resonances of U-R and C-R derivatives aligned to allow comparison of the peak widths, showing the effective coupling strength between molecules and Au electrodes.

To investigate the impact of side groups on the LUMO energies of these analogs, we exploit cyclic voltammetry (CV) measurements as a proxy for the energy of the LUMO. The reduction waves for each analog in both the U-R and C-R series show that there is a single-electron transfer event that results in the reduction of the central carbocation to the neutral radical (see Figure S2). In Figure 3a, we show the LUMO levels of all analogs derived from CV reduction waves.<sup>24,25</sup> For both the U-R and C-R series, as the R group on the pendant substituent becomes increasingly more  $\pi$ -electron donating (CF<sub>3</sub> < H < SEt < NEt<sub>2</sub>), the carbocation becomes more shielded, and the LUMO energy increases. Similar trends in the calculated LUMO energies are observed in DFT calculated LUMO energies shown in Figure 3b. Since the LUMO energy shifts for the U-R and C-R series were similar (see Figures 3a and 3b), the large difference in the

conductance trends cannot simply be attributed to the shift of the LUMO resonance relative to  $E_F$ . These compounds were also characterized by UV-Visible spectroscopy, which can be found in Figure S3.

To better understand the charge transport mechanisms of these molecules and explain the greater conductance tuning factor for the U-R series (~450) compared to the C-R series (~6), we calculate the DFT based transmission functions for both series (Figure 3c and 3d, see SI for details).<sup>26-30</sup> In each of the transmission functions, we observe Fano resonances (a sharp dip and spike) below  $E_F$ . These Fano resonances are the result of a destructive interference between the occupied orbitals localized on the pendant phenyl ring and the molecular backbone. We see that the Fano dips are much closer to  $E_F$  in the U-R series (i.e.,  $\varepsilon_p \sim 1.0$ -1.4 eV) compared to the C-R series (i.e.,  $\varepsilon_p \sim 1.6$ -2.2 eV), thus having a greater impact on the LUMO energies. Additionally, the separation between the Fano dips and spikes increases going from more electron-withdrawing to electron-donating substituents, an effect that is more prominent in the U-R series compared to the C-R series. Next, we note that the resonance that is closest to  $E_F$  is the LUMO for all analogs, which is to be expected for cations. For the U-R series, we see that the LUMO energies shift away from  $E_F$ , while its width decreases as the electron donating ability of the R group increases. By contrast, for the C-R series both the shift in the LUMO energies and the change in resonance width are not as significant, despite the LUMO changing across both series by roughly the same amount, as shown in Figures 3a and 3b. Therefore, changes in molecular conductance cannot simply be attributed to a gating of the LUMO in an isolated molecule, but rather to the impact of the Fano resonance on both the position and width of the LUMO, which is determined by the coupling of pendant orbital to the conduction orbital (t in eq. 2).

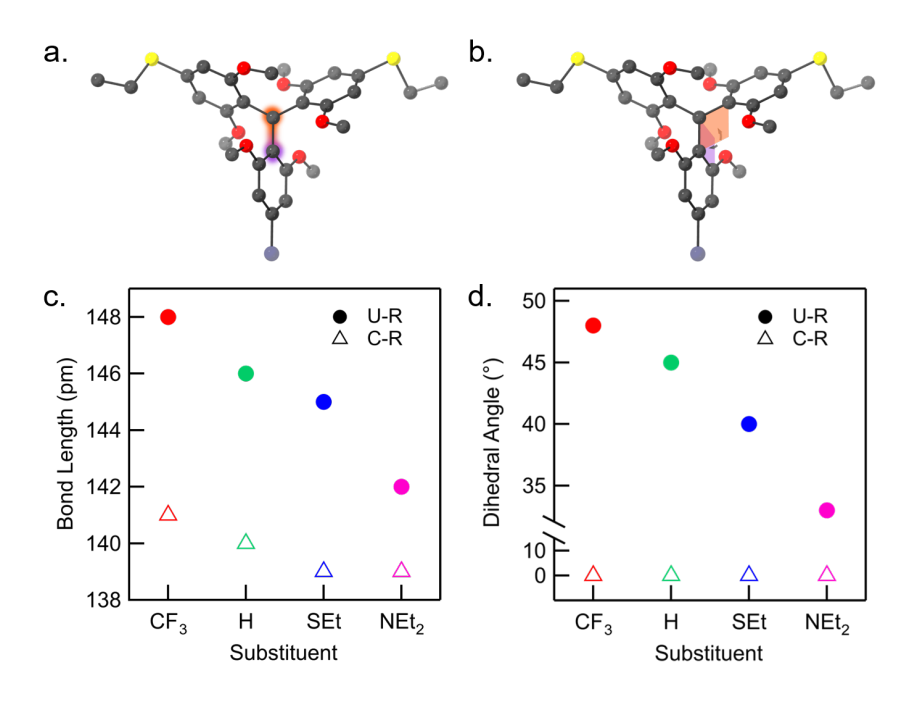


Figure 4. Illustration of (a) the length and (b) dihedral angle of the bond between the pendant phenyl ring and the molecular backbone in a U-R molecule. The dihedral angle is measured between the purple and orange intersecting planes. (Illustration of C-R molecule is omitted here.) (c) Bond length and (d) dihedral angle measured from DFT optimized isolated cation geometries of both U-R and C-R series.

To explore how the structural modifications affect the coupling of the pendant orbital to the conduction orbital, we investigate the structures of the isolated analogs optimized by DFT calculations.<sup>31-33</sup> Since Fano resonances arise from the coupling (t) between the localized orbital on the pendant phenyl ring and the delocalized conducting orbital on the molecular backbone, we focus on the bond that bridges these moieties. We first look at the bond length (illustrated in Figure 4a), which is a proxy for the degree of conjugation (i.e., the shorter the bond the more the conjugation). For the U-R series, as we increase the electron donating ability of the pendant phenyl ring, the bond length decreases (Figure 4c), i.e., the coupling t between the pendant phenyl ring and the conduction channel increases. Similarly, dihedral torsion angle (illustrated in Figure 4b) also indicates the strength of this coupling such that a smaller dihedral angle indicates a stronger orbital overlap and coupling strength. Again, going from CF<sub>3</sub> to NEt<sub>2</sub>, we see that the

dihedral angle decreases (Figure 4d). As we change the nature of the pendant group, we alter the pendant coupling t which narrows the LUMO, thus explaining the experimental conductance trend for the U-R series. As for the C-R series with locked rigid structures, the dihedral angle and bond length do not change significantly when the electron withdrawing or donating nature of the substituent is changed (Figures 4c and 4d). This leads to an energetically deeper Fano resonance which impacts the LUMO position and width, resulting in a much weaker chemical gating effect on molecular conductance.

In conclusion, we have shown that single-molecule conductance can be effectively tuned by chemical gating with a pendant substituent. These pendant substituents, with MOs that are decoupled from the leads give rise to a Fano resonances in the transmission due to a destructive quantum interference effect that greatly enhances the change in conductance that can be achieved by substituent gating. Using this new design principle, we are able to tune molecular conductance by up to a factor of 450 without altering the molecular conductance pathway. This study charts a clear path to single-molecule transistors that can be effectively gated, with highly modular single-molecule conductance and transport properties.

#### ASSOCIATED CONTENT

# **Supporting Information**

Theoretical models, synthetic procedures, characterization data, measurement and calculation details, and additional data.

## **AUTHOR INFORMATION**

# **Corresponding Authors**

Colin Nuckolls – Department of Chemistry, Columbia University, New York, New York 10027, United States; orcid.org/0000-0002-0384-5493; Email: <a href="mailto:cn37@columbia.edu">cn37@columbia.edu</a>

**Latha Venkataraman** – Department of Chemistry and Department of Applied Physics and Applied Mathematics, Columbia University, New York, New York 10027, United States; orcid.org/0000-0002-6957-6089; Email: lv2117@columbia.edu

## Authors

Claudia R. Prindle – Department of Chemistry, Columbia University, New York, New York 10027, United States; orcid.org/0009-0008-4111-3550; Email: <a href="mailto:crp2163@columbia.edu">crp2163@columbia.edu</a>

**Wanzhuo Shi** – Department of Chemistry, Columbia University, New York, New York 10027, United States; orcid.org/0000-0003-2103-9185; Email: <a href="ws2637@columbia.edu">ws2637@columbia.edu</a>

**Liang Li** – Department of Chemistry, Columbia University, New York, New York 10027, United States; orcid.org/0000-0003-3890-7276; Email: <a href="mailto:ll3332@columbia.edu">ll3332@columbia.edu</a>

**Jesper Dahl Jensen** – Nano-Science Center and Department of Chemistry, University of Copenhagen, Universitetsparken 5, 2100 Copenhagen, Denmark; Email: jdj@chem.ku.dk

**Bo W. Laursen** – Nano-Science Center and Department of Chemistry, University of Copenhagen, Universitetsparken 5, 2100 Copenhagen, Denmark; orcid.org/0000-0002-1120-3191; Email: <a href="mailto:bwl@nano.ku.dk">bwl@nano.ku.dk</a>

Michael L. Steigerwald – Department of Chemistry, Columbia University, New York, New York 10027, United States; orcid.org/0000-0001-6337-2707; Email: <a href="mls2064@columbia.edu">mls2064@columbia.edu</a>

## **Author Contributions**

<sup>†</sup>C.R.P. and W.S. contributed equally.

#### ACKNOWLEDGMENT

C.R.P. was supported by a National Defense Science and Engineering Graduate Fellowship. W.S. was supported by the U.S.-Israel Binational Science Foundation Award 2020327. L.L was supported by the National Science Foundation Award NSF DMR-2241180.

## **REFERENCES**

- (1) Evers, F.; Korytár, R.; Tewari, S.; van Ruitenbeek, J. M., Advances and challenges in single-molecule electron transport, *Rev. Mod. Phys.*, **2020**, 92, 035001.
- (2) Yoshizawa, K., An Orbital Rule for Electron Transport in Molecules, *Acc. Chem. Res.*, **2012**, 45, 1612-1621.
- (3) Cardamone, D. M.; Stafford, C. A.; Mazumdar, S., Controlling quantum transport through a single molecule, *Nano Lett.*, **2006**, 6, 2422-2426.
- (4) Andrews, D. Q.; Solomon, G. C.; Van Duyne, R. P.; Ratner, M. A., Single Molecule Electronics: Increasing Dynamic Range and Switching Speed Using Cross-Conjugated Species, *J. Am. Chem. Soc.*, **2008**, 130, 17309-17319.
- (5) Datta, S., Electrical resistance: an atomistic view, *Nanotechnology*, **2004**, 15, S433-S451.
- (6) Datta, S., *Quantum transport : atom to transistor*. Cambridge University Press: Cambridge, UK; New York, 2005; p xiv, 404 p.
- (7) Breit, G.; Wigner, E., Capture of slow neutrons, *Phys. Rev.*, **1936**, 49, 0519-0531.
- (8) Schuster, R.; Buks, E.; Heiblum, M.; Mahalu, D.; Umansky, V.; Shtrikman, H., Phase measurement in a quantum dot via a double-slit interference experiment, *Nature*, **1997**, 385, 417-420.
- (9) Su, T. A.; Neupane, M.; Steigerwald, M. L.; Venkataraman, L.; Nuckolls, C., Chemical principles of single-molecule electronics, *Nat. Rev. Mater.*, **2016**, 1, 16002.
- (10) Hammett, L. P., The effect of structure upon the reactions of organic compounds benzene derivatives, *J. Am. Chem. Soc.*, **1937**, 59, 96-103.
- (11) Ivie, J. A., et al., Correlated Energy-Level Alignment Effects Determine Substituent-Tuned Single-Molecule Conductance, *Acs. Appl. Mater. Inter.*, **2021**, 13, 4267-4277.

- (12) Venkataraman, L.; Park, Y. S.; Whalley, A. C.; Nuckolls, C.; Hybertsen, M. S.; Steigerwald, M. L., Electronics and chemistry: Varying single-molecule junction conductance using chemical substituents, *Nano Lett.*, **2007**, 7, 502-506.
- (13) Liang, X.; Pan, Z. Y.; Go, W.; Mack, J.; Soy, R.; Nyokong, T.; Zhang, Q. C.; Zhu, W. H., Regulating the Single-Molecule Conductance of Corroles by the Substituents on the B-Site, *J. Phys. Chem. C*, **2022**, 126, 21476-21481.
- (14) Lo, W. Y.; Bi, W. G.; Li, L. W.; Jung, I. H.; Yu, L. P., Edge-on Gating Effect in Molecular Wires, *Nano Lett.*, **2015**, 15, 958-962.
- (15) Yin, X.; Zang, Y.; Zhu, L.; Low, J. Z.; Liu, Z. F.; Cui, J.; Neaton, J. B.; Venkataraman, L.; Campos, L. M., A Reversible Single-Molecule Switch based on Activated Antiaromaticity, *Sci. Adv.*, **2022**, 8.
- (16) Li, Z.; Smeu, M.; Afsari, S.; Xing, Y.; Ratner, M. A.; Borguet, E., Single-Molecule Sensing of Environmental pH-an STM Break Junction and NEGF-DFT Approach, *Angew. Chem. Int. Ed.*, **2014**, 53, 1098-1102.
- (17) Lambert, C. J., Basic concepts of quantum interference and electron transport in single-molecule electronics, *Chem. Soc. Rev.*, **2015**, 44, 875-888.
- (18) Wada, M.; Konishi, H.; Kirishima, K.; Takeuchi, H.; Natsume, S.; Erabi, T., Unusual stabilities and reactivities of tris- and bis(2,4,6-trimethoxyphenyl)carbenium salts, *Bull. Chem. Soc. Jpn.*, **1997**, 70, 2737-2741.
- (19) Laursen, B. W.; Krebs, F. C.; Nielsen, M. F.; Bechgaard, K.; Christensen, J. B.; Harrit, N., 2,6,10-tris(dialkylamino)trioxatriangulenium ions. Synthesis, structure, and properties of exceptionally stable carbenium ions, *J. Am. Chem. Soc.*, **1999**, 121, 4728-4728.
- (20) Santella, M.; Della Pia, E.; Sorensen, J. K.; Laursen, B. W., Synthesis and properties of sulfurfunctionalized triarylmethylium, acridinium and triangulenium dyes, *Beilstein J. Org. Chem.*, **2019**, 15, 2133-2141.
- (21) Xu, B. Q.; Tao, N. J., Measurement of single-molecule resistance by repeated formation of molecular junctions, *Science*, **2003**, 301, 1221-1223.
- (22) Venkataraman, L.; Klare, J. E.; Nuckolls, C.; Hybertsen, M. S.; Steigerwald, M. L., Dependence of single-molecule junction conductance on molecular conformation, *Nature*, **2006**, 442, 904-907.
- (23) Capozzi, B.; Xia, J. L.; Adak, O.; Dell, E. J.; Liu, Z. F.; Taylor, J. C.; Neaton, J. B.; Campos, L. M.; Venkataraman, L., Single-molecule diodes with high rectification ratios through environmental control, *Nat. Nano.*, **2015**, 10, 522-527.
- (24) Bredas, J. L.; Silbey, R.; Boudreaux, D. S.; Chance, R. R., Chain-length dependence of electronic and electrochemical properties of conjugated systems: polyacetylene, polyphenylene, polythiophene, and polypyrrole, *J. Am. Chem. Soc.*, **1983**, 105, 6555-6559.
- (25) Parker, V. D., Problem of assigning values to energy changes of electrode reactions, *J. Am. Chem. Soc.*, **1974,** 96, 5656-5659.
- (26) Blum, V.; Gehrke, R.; Hanke, F.; Havu, P.; Havu, V.; Ren, X.; Reuter, K.; Scheffler, M., Ab initio molecular simulations with numeric atom-centered orbitals, *Comp. Phys. Comm.*, **2009**, 180, 2175-2196.
- (27) Arnold, A.; Weigend, F.; Evers, F., Quantum chemistry calculations for molecules coupled to reservoirs: Formalism, implementation, and application to benzenedithiol, *J. Chem. Phys.*, **2007**, 126, 174101.
- (28) Bagrets, A., Spin-polarized electron transport across metal—organic molecules: a density functional theory approach, *J. of Chem. Theory Comp.*, **2013**, 9, 2801-2815.
- (29) Perdew, J. P.; Burke, K.; Ernzerhof, M., Generalized gradient approximation made simple, *Phys. Rev. Lett.*, **1996**, 77, 3865.
- (30) Wilhelm, J.; Walz, M.; Stendel, M.; Bagrets, A.; Evers, F., Ab initio simulations of scanning-tunneling-microscope images with embedding techniques and application to C 58-dimers on Au (111), *Phys. Chem. Chem. Phys.*, **2013**, 15, 6684-6690.
- (31) Bochevarov, A. D., et al., Jaguar: A high-performance quantum chemistry software program with strengths in life and materials sciences, *Int. J. of Quant. Chem.*, **2013**, 113, 2110-2142.

- (32) Becke, A. D., Density-Functional Thermochemistry .3. The Role of Exact Exchange, *J. Chem. Phys.*, **1993**, 98, 5648-5652.
- (33) Lee, C. T.; Yang, W. T.; Parr, R. G., Development of the Colle-Salvetti Correlation-Energy Formula into a Functional of the Electron-Density, *Phys. Rev. B*, **1988**, 37, 785-789.

# TOC

